Reversing exchange bias in thermally assisted magnetic random access memory cell by electric current heating pulses

C. Papusoi,[1,a)] R. C. Sousa,[1] B. Dieny,[1] I. L. Prejbeanu,[2] Y. Conraux,[2] K. Mackay,[2] and J. P. Nozières[2]
[1]*Spintec, URA 2512 CEA/CNRS, 17 r. des Martyrs, 38054 Grenoble, France*
[2]*Crocus Technology, 5 Place Robert Schumann, BP 1510, 38025 Grenoble, France*

(Received 13 February 2008; accepted 28 April 2008; published online 10 July 2008)

The temperature required to set the exchange bias of a ferro/antiferromagnetic (F/AF) storage bilayer as a function of the heating pulse width was studied on magnetic tunnel junctions (MTJs) of thermally assisted magnetic random access memories. Heating is produced by a pulse of electric current flowing through the junction. For sufficiently long heating pulse (>20 ns), a quasiequilibrium temperature profile is reached in the MTJ. In this stationary regime, a relationship between the temperature of the storage layer and the power of the pulse was established by using an Arrhenius–Néel model of thermal relaxation. The introduction of thermal barriers between the junction tunnel barrier and the electrodes allows a significant reduction of the power required to achieve a given temperature rise of the storage layer. When the heating pulse duration is reduced from 1 s to 2 ns, the heating power required for setting the F/AF storage bilayer increases by about 80%. This experimental observation is quantitatively interpreted by combining the Arrhenius–Néel model with thermodynamic simulations of heat diffusion with source term given by the experimentally known heating power dissipated in the tunnel barrier by Joule effect. © *2008 American Institute of Physics*. [DOI: 10.1063/1.2951931]

I. INTRODUCTION

Exchange bias phenomenon,[1,2] leading to the pinning of the magnetization of a ferromagnetic (F) layer in contact with an antiferromagnetic (AF) layer, has been extensively used in spin valves, magnetic tunnel junctions (MTJs) and other spintronic devices to create reference direction for the spin of the electrons.[3] The same principle is used in thermally assisted magnetic random access memory (TAMRAM), where each memory element consists of a MTJ comprising a storage layer exchange biased by an AF.[4–7] In this case, the magnetization direction of the F/AF storage layer is set by heating the tunnel junction to a setting temperature T_{set} with an electric current pulse flowing through the junction in the direction perpendicular-to-plane, in the presence of a magnetic field. The applied field stands during the natural cooling of the MTJ layers back to room temperature (RT) $T_{RT}=300$ K, subsequent to the suppression of the heating pulse. Cooling of the F/AF storage layer with the F layer oriented in the applied field direction freezes the AF state and creates an exchange bias along the applied field direction. The setting temperature for writing a TAMRAM must be larger than the *blocking temperature* (T_B) of the F/AF storage layer for the corresponding duration of the heating pulse δ. The relationship between blocking temperature and heating pulse duration can be established as follows. Let us assume that the exchange bias acting on the storage layer H_{EX} is initially set in the positive direction (meaning a loop shift in the positive direction) to H_{EX}^{set} by cooling the F/AF system from a temperature higher than the Néel temperature T_N down to T_{RT} in the presence of a negative applied field $-H_{set}$, high enough to orient the F layer along to its direction. In attempt to reverse the direction of H_{EX}, a second heating is performed at a temperature $T_{AF}>T_{RT}$ during the time interval δ, followed by cooling to T_{RT} in the presence of a positive applied field H_{set}. In these experiments, it is assumed that the duration of the transient regimes of temperature variation from T_{RT} to T_{AF} and from T_{AF} to T_{RT} (typically ~20 ns) are much shorter than δ (longer than 100 ns) so that the temperature can be considered as constant during δ. This quasiequilibrium temperature is determined by a balance between the heating power dissipated at the tunnel barrier and the heat flow diffusing towards bottom and top electrodes which constitute heat sinks. As a result of the heating pulse of duration δ, the exchange bias decreases to a value $H_{EX}(T_{AF},\delta)$. The blocking temperature T_B is the temperature reached by the F/AF bilayer during δ for which a decrease of the exchange bias from H_{EX}^{set} to $H_{EX}(T_{AF}=T_{AF}^{W}\equiv T_B,\delta)=H_{EX}^{W}=0$ is observed. The goal of this study was to measure and interpret the strong dependence of T_B on the heating pulse duration in a fairly large window of heating time ranging from 2 ns up to 1 s. For this purpose, experiments on TAMRAM devices were performed. In these systems, the duration and amplitude of the temperature step can be easily controlled by the width δ and power P_{HP} of the electric heating pulse flowing through the junction. The experimental setup and the procedure for measuring the power of the electric pulse P_{HP}^{W} leading to $H_{EX}=H_{EX}^{W}$, which is the TAMRAM writing criterion, are described below. In the experiments, we do not have direct access to the temperature of the F/AF bilayer. Therefore, the temperature profile of the junction subsequent to the application of an electric heating pulse and in particular the temperature at the F/AF bilayer location was

[a)]Electronic mail: cristian.papusoi@cea.fr.

 © 2008 American Institute of Physics

calculated by solving the heat diffusion equation (HDE) for the geometry and structure of the investigated device. The heat source term in the HDE is the Joule dissipation in the tunnel barrier given by the measured power of the electric pulse P_{HP}^{W}. The HDE approach involves a number of thermodynamic parameters, including the specific heat capacities and thermal conductivities of all layers comprised in the MTJ and electrodes. Their values may be different for patterned thin films than for bulk materials. For validating the parameter values used in HDE simulations, a second method to determine the temperature of the storage layer as a function of the electric pulse power, based on the temperature and time dependence of H_{EX} calculated by an Arrhenius–Néel (A-N) model of thermal relaxation, was used as a reference. This model involves a number of structural and magnetic parameters (AF grain size, AF anisotropy, and interatomic interfacial F/AF coupling) which were determined from quasistatic measurements of exchange bias and coercivity versus temperature and direct structural observations. Once the magnetic parameters of the F/AF storage layer were determined, the A-N model was used to calculate the temperature T_B, i.e., the amplitude of a temperature pulse applied to the F/AF storage layer leading to the same threshold of exchange bias $H_{EX}^{W}=0$ as the experimental electric pulse of power P_{HP}^{W}.

In a first approach, considering the shortness of the transient regime of temperature variation ($\sim$20 ns) when the heating current pulse is switched on or off, the AF temperature variation during the application of the electric pulse was assumed to be rectangular, having the same width δ as that of the electric pulse. Agreement over a large interval of pulse widths, extending from 20 ns to 1 s, was obtained between the result of HDE simulations and the result of the A-N model regarding the temperature of the AF layer $T_{AF}^{W}=T_B$ at $t=\delta$. In a second approach, we took into account the finite heating/cooling times required by the junction to reach a stationary temperature regime. These transient regimes play a role for short heating pulse widths, typically below 20 ns. To treat this case, the A-N model was adapted to calculate H_{EX} at the end of an arbitrarily shaped temperature pulse. The time dependence of the AF temperature during and after the application of an electric pulse of power P_{HP}^{W} and width δ was calculated by HDE simulations and then introduced in the A-N model to calculate H_{EX} at the end of the pulse. This approach improved the agreement between the combined HDE/A-N models and the experimental results in the range of short pulse widths 2–20 ns. The matching between the combined HDE/A-N model and the experiments evidenced an increase of T_B by almost 80% when the electric pulse duration decreases from 1 s down to 2 ns. The importance of this conclusion is twofold. On one hand, it confirms that the difference between T_B and T_N in thin F/AF bilayers is a consequence of thermal activation. On the other hand, it suggests that the power required to set the exchange bias by heating with short electric pulses could be decreased by using materials with lower T_N. The important values reached by the temperature in the nanosecond pulse width regime were enabled by the insertion in the junction stack of layers having a low thermal conductivity, playing the role of thermal barriers.

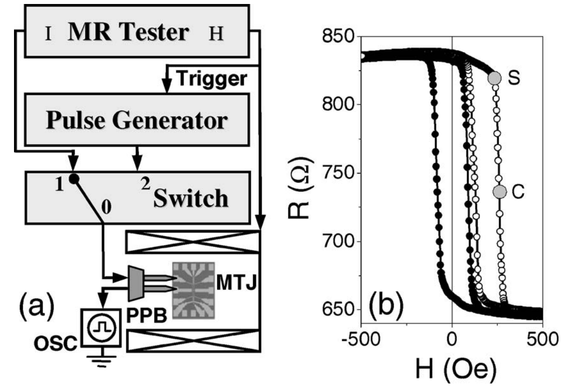

FIG. 1. (a) Experimental setup. (b) Writing test on a thermally assisted MRAM by the simultaneous application of an electric pulse of power P_{HP} and a magnetic field pulse of amplitude H_{set}: saturation of the exchange bias to H_{EX}^{set} using $P_{HP}^{set}=2$ mW, $\delta_{set}=1$ ms, and $H_{set}=-500$ Oe (○) and exchange bias reversal to $H_{EX}^{W}=0$ Oe using $P_{HP}^{W}=1.1$ mW, $\delta=1$ ms, and $H_{set}=+500$ Oe (●).

II. EXPERIMENTAL

The MRAM device subject to our investigation contained a MTJ with a $Co_{80}Fe_{20}$ 1.5/$Ni_{80}Fe_{20}$ 3 nm storage layer, exchange biased by a 5 nm thin $Ir_{20}Mn_{80}$ AF layer. The reference layer was pinned by a $Pt_{36}Mn_{64}$, high T_N, AF layer and the complete stack had the following structure: bottom electrode/Ta 50/$Pt_{36}Mn_{64}$ 20/$Co_{80}Fe_{20}$ 2.5/Ru 0.8/$Co_{80}Fe_{20}$ 3.0/AlO_x 0.5/$Co_{80}Fe_{20}$ 1.5/$Ni_{80}Fe_{20}$ 3/$Ir_{20}Mn_{80}$ 5 nm/top electrode. Top and bottom electrodes were made of Cu 250 nm and Ta 5/Al 20/Ta 90/Al 300 nm, respectively. The junction was patterned in an elliptical shape of 450 nm long and 250 nm short axes. The saturation magnetization of the storage layer was $M_S=910$ emu/cm^3, leading to a theoretical shape anisotropy $K_D=1.59\times10^4$ ergs/cm^3. In order to set the exchange bias of the reference and storage layers, a heating of the junction up to $T=350$ °C was performed, followed by cooling in the presence of an applied field $H=5$ kOe.

Our experimental setup is presented in Fig. 1(a). Setting of the storage layer H_{EX} was performed by connecting the probe pin board (PPB) to the pulse generator (0–2 in Fig. 1(a)), applying a step of magnetic field $H_{set}=\pm500$ Oe delivered by an electromagnet and during field application, sending a heating electric pulse of amplitude U and width δ provided by the pulse generator through the MTJ. The properties of the F/AF storage layer (coercivity H_C and exchange bias H_{EX}) were measured at RT immediately after suppression of the field, by connecting PPB to magnetoresistance (MR) tester [0–1 in Fig. 1(a)], from quasistatic MR hysteresis cycle using 40 mV bias voltage, as illustrated in Fig. 1(b). At this bias voltage, the heating of the MTJ is negligible. The measurement of an MR cycle with field varying between ±500 Oe takes $t_{MEAS}=50$ ms. In order to minimize any exchange bias training effects, 50 MR cycles were performed before the actual measurement. The power of the electric pulse was calculated as $P_{HP}=(2U\text{-}Z_{PG}I\text{-}U_{OSC})I$, where $I=U_{OSC}/Z_{OSC}$ is measured by an oscilloscope (OSC) of impedance $Z_{OSC}=50\ \Omega$ and $Z_{PG}=50\ \Omega$ is the output impedance of the pulse generator. The procedure for setting H_{EX} to a specific threshold, e.g., $H_{EX}^{W}=0$ Oe as shown in Fig. 1(b), consisted in the application of an electric pulse of

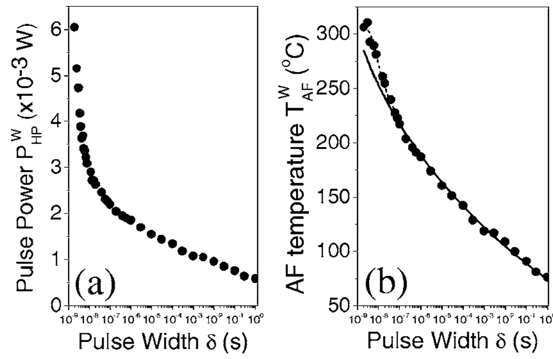

FIG. 2. (a) Power of the electric pulse P_{HP}^{W} required to reduce the exchange bias, initially set to $H_{\mathrm{EX}}^{\mathrm{set}}$, to the threshold value $H_{\mathrm{EX}}^{W}=0$ Oe, as a function of the pulse width δ. (b) Temperature T_{AF}^{W} reached by the AF layer at the end ($t=\delta$) of an electric pulse of power $P_{\mathrm{HP}}^{W}(\delta)$ as a function of the pulse width δ, calculated by the HDE model (symbols) and by the A-N model using the assumption of a rectangular temperature pulse (solid line) or the temperature variation pattern calculated by the HDE model (dashed line).

power P_{HP}, duration δ, triggered by a field pulse $H_{\mathrm{set}}=+500$ Oe, the value of P_{HP} being progressively increased until the condition $H_{\mathrm{EX}}=H_{\mathrm{EX}}^{W}$ was fulfilled. The corresponding power of the electric pulse was P_{HP}^{W}. This procedure was repeated for various pulse durations δ in the range of 2 ns–1 s, the measured $P_{\mathrm{HP}}^{W}(\delta)$ being plotted in Fig. 2(a). Before setting H_{EX}, the previous magnetic state of the storage layer was erased by saturating H_{EX} to $H_{\mathrm{EX}}^{\mathrm{set}}$. For this purpose, an electric pulse of power $P_{\mathrm{HP}}^{\mathrm{set}}=2$ mW, width $\delta_{\mathrm{set}}=1$ ms, triggered by a magnetic field pulse of amplitude $H_{\mathrm{set}}=-500$ Oe, was applied to the junction. The value of $P_{\mathrm{HP}}^{\mathrm{set}}$ was established by monitoring the dependence of H_{EX} on P_{HP} for progressively increasing values of the latter and for both orientations of the applied field H_{set} until $H_{\mathrm{EX}}(H_{\mathrm{set}}=-500\text{ Oe})=-H_{\mathrm{EX}}(H_{\mathrm{set}}=+500\text{ Oe})=H_{\mathrm{EX}}^{\mathrm{set}}$.

In order to quantify the magnetic parameters of the F/AF storage layer, the following experiment was performed. After setting of the exchange bias by cooling from 350 °C in the presence of the applied field $H=5$ kOe, the junction was heated from RT up to 190 °C by using a heating chuck and the exchange bias H_{EX} and coercivity H_C of the storage layer were measured from quasistatic MR loops at several intermediate temperatures, the results being plotted in Fig. 3. As

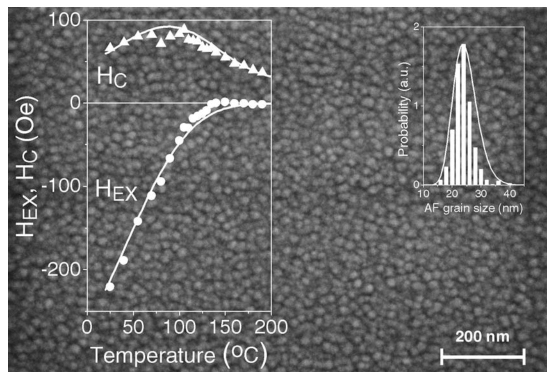

FIG. 3. Experimental [symbols, H_{EX} (●) and H_{C} (▲)] and calculated (solid line) $H_{\mathrm{EX}}(\mathrm{T})$ and $H_{\mathrm{C}}(\mathrm{T})$ of the storage layer. (Inset) IrMn grain size distribution (bars) from SEM image (background) and derived from the A-N model.

explained below, these data were interpreted by an A-N model from which magnetic and structural parameters such as AF anisotropy, atomic interfacial F/AF coupling, and grain size can be derived. The grain size was then verified by direct electron microscopy observation.

III. THEORY

In order to calculate the temperature profile of the MTJ during the application of a heating electric pulse of power P_{HP} and width δ, a thermodynamic approach has been used, based on the heat diffusion equation of general expression

$$C\rho\frac{\partial T}{\partial t}-\nabla k\,\nabla T=Q, \tag{1}$$

where C is the specific heat capacity of the material subjected to Joule heating, ρ is its mass density, k is its thermal conductivity, Q is the heating power per unit volume applied to the material, T is the temperature, and t is the time. This equation was solved for each layer of the MTJ, using the appropriate geometry and temperature boundary conditions, by using the three-dimensional (3D) finite element solver of the heat diffusion equation COMSOL. Conducting heat transfer was assumed between adjacent layers, thermal insulation condition on the noncontacted surfaces, and constant RT temperature condition was used for the end surfaces of the electrodes. The thermodynamic parameters of the model were the thermal conductivities k and specific heat capacities C of all the junction layers, including the electrodes and the $\mathrm{SiO_2}$ insulator between the top and bottom electrodes. For the layers made of pure elements, we have used the bulk values for k and C.[8] For the alloys, specific heat capacities were estimated according to $C=C_M/(\rho V_M)$, where the molar heat capacity takes similar values for all metals $C_M\approx 26$ J/(K mol), $V_M=(N_A V_U)/Z$ is the molar volume of the alloy, V_U is the volume of the crystalline lattice unit cell, Z is the number of atoms per lattice unit cell, and $\rho=Z\Sigma_i(n_iA_i)/(N_AV_U)$ is the mass density, and n_i and A_i being the atomic concentration and atomic masses of the constituents, respectively. The values of k for the alloys were calculated based on the Widemann–Franz law of electronic thermal conductivity $k=LT/\rho_e$ where $L=2.510^{-8}$ WΩ/K^2 is the Lorentz number, ρ_e is the electrical resistivity, and T is the temperature. The values of ρ_e measured at RT were used and, in a first approximation, the temperature dependence of C and k were neglected. Since the layer with the highest electrical resistance is the $\mathrm{AlO_x}$ tunnel barrier, the energy of the electric pulse was assumed to be dissipated by Joule effect in the tunnel barrier. Accordingly, Q in Eq. (1) is zero for all the layers of the junction except for the tunnel barrier where $Q=P_{\mathrm{HP}}^{W}/(a_{\mathrm{AlO}_x}A_{\mathrm{AlO}_x})$, where a_{AlO_x}, A_{AlO_x} are the thickness and surface of the tunnel barrier. In the simulation, the heating pulse of duration δ and corresponding power $P_{\mathrm{HP}}^{W}(\delta)$ on the writing curve in Fig. 2(a) was applied at $t=0$. A first simulation was performed for $0<t<\delta$, corresponding to the heating stage. For illustration, the calculated temperature map throughout a MTJ pillar submitted to a step of heating current of power $P_{\mathrm{HP}}^{W}(\delta=16\text{ ns})$ at $t=\delta=16$ ns after onset of the heating current is presented in Fig. 4(a), together with a cross

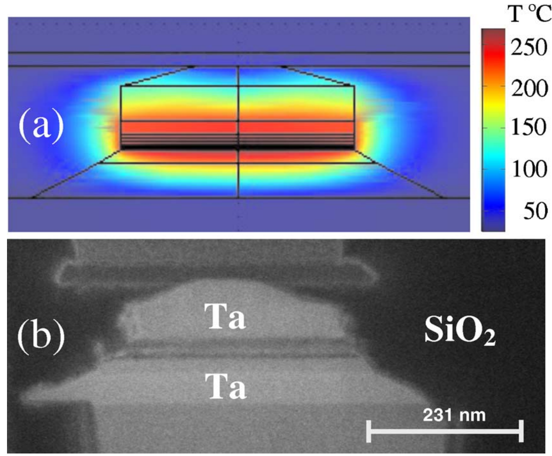

FIG. 4. (Color online) (a) Temperature profile of the MRAM device at the end ($t=\delta$) of an electric pulse of power P_{HP}^{W} ($\delta=16$ ns), as calculated by the HDE model. (b) Cross section TEM image of the MRAM device.

section TEM image of the real device in Fig. 4(b). The temperature T_{AF}^{W} reached by the AF layer at the end of a heating pulse of duration δ, averaged over the thickness of the AF layer, is plotted in Fig. 2(b) as a function of δ and corresponding power P_{HP}^{W}. The simulation was continued for $t>\delta$, i.e., during the cooling stage, in order to obtain the complete shape of the temperature pulse generated by the electric pulse. The rise time of the pulse generator was taken into account by assuming a time dependent shape of the heating pulse power, of the form $P_{\mathrm{HP}}^{W}\min(1,t^2/t_R^2)$ for the heating stage and $P_{\mathrm{HP}}^{W}\max[0,1-(t-\delta)^2/t_R^2]$ for the cooling stage, where $t_R=0,8$ ns is the rise time. For illustration, the calculated AF temperature pulse resulting from the application of an electric pulse of power $P_{\mathrm{HP}}^{W}(\delta=16$ ns) is presented in Fig. 5(a), together with the temperature profile of the MRAM stack sandwiched between the two electrodes at $t=\delta=16$ ns in Fig. 5(b).

In order to confirm the dependence $T_{\mathrm{AF}}^{W}(\delta)$ calculated by thermodynamic simulations in Fig. 2(b) and check that our choice of thermodynamic parameters (specific heat and thermal conductivity) was correct, we used the temperature dependent magnetic properties of the F/AF storage layer. The

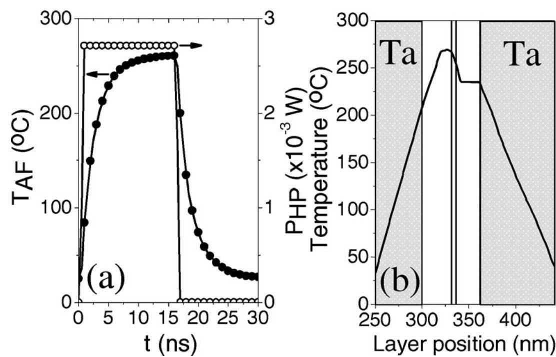

FIG. 5. (a) Temperature variation pattern of the AF layer $T_{\mathrm{AF}}(t)$ (solid symbols) during the application of an electric pulse of power P_{HP}^{W} ($\delta=16$ ns) (empty symbols), as calculated by the HDE model. (b) Temperature profile of the stack between the two electrodes at $t=\delta$, resulting from the application of an electric pulse of power P_{HP}^{W} ($\delta=16$ ns), as calculated by the HDE model.

exchange bias set by a temperature pulse of amplitude T_{AF} and duration δ can be calculated by an A-N model.[9–12] This model was used to calculate the amplitude T_{AF}^{W} of a temperature pulse, of equal duration to that of the experimental electric pulse δ, that sets H_{EX} to the writing threshold value $H_{\mathrm{EX}}=H_{\mathrm{EX}}^{W}=0$ Oe. In order to determine the parameters used in the A-N model, the temperature dependences of H_{EX} and H_C plotted in Fig. 3 were fitted. The exchange coupling energy per unit F/AF contact surface was written $J_E=J_{\mathrm{INT}}/(a_0D)$,[12] where J_{INT} is the exchange interaction energy between a pair of F/AF atoms, $a_0=2.5$ Å is the mean AF atomic distance at the F/AF interface, and D is the AF grain diameter. Following Ref. 12, the temperature dependences of the AF anisotropy K_{AF} and J_{INT} are assumed to be given by $K_{\mathrm{AF}}(T)=K_{\mathrm{AF}}^0(1-T/T_N)^{0.99}$ and $J_{\mathrm{INT}}(T)=J_{\mathrm{INT}}^0(1-T/T_N)^{0.33}$, where $T_N=350$ °C is the Néel temperature of the AF. According to the theory developed in Refs. 10 and 11,

$$H_{\mathrm{EX}}=\frac{J_{\mathrm{INT}}}{a_0M_Sa_F}\frac{1}{I}\int_{\max(D_0,D^*)}^{\infty}(P_- - P_+)DG(D)\mathrm{d}D, \quad (2)$$

$$H_C=\frac{2K_F}{M_S}+\frac{J_{\mathrm{INT}}}{a_0M_Sa_F}\frac{1}{I}\int_{D^*}^{\infty}(P_- + P_+ - 1)DG(D)\mathrm{d}D, \quad (3)$$

where K_F is the uniaxial anisotropy constant of the F layer, a_F is the F layer thickness, and $I=\int_0^\infty D^2G(D)dD$ where $G(D)$ is the AF grain size distribution. The diameter $D_0=J_{\mathrm{INT}}/(K_{\mathrm{AF}}a_{\mathrm{AF}}a_0)$, where a_{AF} is the AF layer thickness, separates the AF grains that are switched ($D<D_0$) from those that are not switched ($D>D_0$) during the rotation of the F layer moment, assuming that the latter is an instantaneous event. In Eqs. (2) and (3), P_+, P_- represent the occupation probabilities of the AF grain energy minimum in the direction [positive (+) or negative (−)] of the F layer just before switching the F layer in the opposite direction, given by Eqs. (20) and (22) of Ref. 10 which can be expressed in a more compact form as

$$P_+=1-[1-P_\infty(1-e^{-t/\tau})]\sum_{i=0}^{2n-2}[(-1)^ie^{-it/\tau}] + P_0e^{-(2n-1)t/\tau}, \quad (4)$$

$$P_-=1-[1-P_\infty(1-e^{-t/\tau})]\sum_{i=0}^{2n-1}[(-1)^ie^{-it/\tau}]-P_0e^{-2nt/\tau}, \quad (5)$$

where τ is the AF grain relaxation time,

$$\tau=1\bigg/\left\{f_0\sum_{\pm}\exp\left[\frac{-\Delta E_\pm}{k_BT}\right]\right\}, \quad (6)$$

and

$$\Delta E_\pm=K_{\mathrm{AF}}a_{\mathrm{AF}}D^2\left(1\mp\frac{J_{\mathrm{INT}}}{2DK_{\mathrm{AF}}a_{\mathrm{AF}}a_0}\right)^2 \quad (7)$$

are the energy barriers to reversal of the AF grain uncompensated moment from an antiparallel orientation to that of the F layer to a parallel orientation (+) and vice versa (−), f_0

$\cong 10^9$ s^{-1}, $t \approx t_{MEAS}/2$ is the time the F layer is oriented in either direction during the measurement of the hysteresis curve, $n=50$ is the number of hysteresis cycles performed at the measurement temperature T prior to measuring H_{EX} and H_C, $P_\infty = 1/\{1+\exp[-2J_{INT}D/(a_0 k_B T)]\}$ and $P_0 = P_+(t=0,n=1)$ is the initial occupation probability before the hysteresis measurement. In Eqs. (2) and (3) the diameter D^* separates the AF grains that are relaxing ($D<D^*$) from those preserving their orientation ($D>D^*$) during the rotation of the F layer moment, by taking into account the experimental time scale of the F layer switching. If one assumes, as in Refs. 10 and 11, that switching of the F layer is an instantaneous event then $D^*=0$, i.e., all the AF grains having a relaxation time $\tau < t_{MEAS}/2$, which switch during the F/AF hysteresis cycles, contribute to the coercivity of the F/AF bilayer. This assumption leads to reasonable values for H_{EX} but it usually overestimates H_C. Experimentally, the switching of the F layer occurs over a finite time interval, e.g., $t_{SW}=t_C-t_S \cong 0.5$ ms as shown in Fig. 1(b), allowing for a fraction of the AF grains to relax *during* the switching of the F layer. This effect can be corrected for in Eqs. (2) and (3) by introducing the diameter D^*, representing the upper AF grain diameter that reaches thermal equilibrium during the switching of the F layer. The value of D^* can be estimated according to

$$t_{SW} = (1/f_0)\exp\left\{\frac{K_{AF}a_{AF}D^{*2}}{k_B T}[1 - J_{INT}/(2K_{AF}a_{AF}a_0 D^*)]^2\right\},$$

which is the expression of the AF relaxation time for a perpendicular orientation of the F layer to the easy axis. Let us briefly describe the contribution of various ranges of AF grain diameters to H_{EX} and H_C in the following:

- The AF grains of diameters $D<D_0$ are switched during the coherent switching of the F layer and contribute only to H_C. One may estimate the maximum contribution of this fraction of grains to H_C by assuming that their uncompensated moments remains parallel to the F magnetization. This assumption leads to an increase of H_C by

  $$\frac{2K_{AF}a_{AF}}{M_S a_F}\frac{1}{I}\int_0^{D_0} D^2 F(D)\mathrm{d}D \text{ . Ref.(11)}$$

  It can be shown that this contribution is negligible with respect to the experimental values of H_C.
- The AF grains of diameter in the range $D_0<D<D^*$ are also contributing only to H_C. However, their contribution could be neglected to a good approximation, since the occupation probabilities of the two energy minima of these AF grains approach very fast the value 0.5 with increasing diameter, i.e., they could be in either of the two minima with equal probability.
- Grains with diameters $D^*<D<D^{**}$, where D^{**} is the solution of equation $\tau = t_{MEAS}/2$, are relaxing during the time interval when the F layer is oriented in either direction along the easy axis. They also contribute only to H_C and their contribution is accounted for in Eq. (3).
- Grains with diameters $D>D^{**}$ are only participating to H_{EX}, since they remain blocked during the entire hysteresis measurement time, their contribution being accounted by Eq. (2).

The $H_{EX}(T)$ and $H_C(T)$ curves were calculated by using Eqs. (2) and (3) with $P_\pm$ given by Eqs. (4) and (5) where $P_0 = P_\infty(T_B^{set})$, T_B^{set} being the solution of $\tau = \delta_{set}$. The fits of the experimental $H_{EX}(T)$ and $H_C(T)$ curves are shown by solid lines in Fig. 3. The following values for the F/AF parameters were obtained from the fit: $t_{SW}=0.5$ ms, $K_F=1.3\times 10^4$ ergs/cm^3, $K_{AF}^0=1.3\times 10^6$ ergs/cm^3, $J_{INT}^0=1.03\times 10^{-14}$ erg leading to RT values $K_{AF}=7.3\times 10^5$ ergs/cm^3 and $J_{INT}=8.5\times 10^{-15}$ erg. The AF grain size distribution $G(D)$ derived from the fit follows a lognormal distribution with $D_m=21$ nm and $\sigma=0.17$, which is in good agreement with that obtained from a scanning electron microscopy (SEM) analysis (Fig. 3).

Next, the A-N model with the parameters found above was used to calculate T_{AF}^W corresponding to $H_{EX}=H_{EX}^W=0$ Oe. As a first approximation for heating pulse duration longer than ~20 ns, the AF temperature variation pattern was assumed to be rectangular, having the same width δ as that of the electric pulse. The exchange bias H_{EX} acting on the storage layer H_{EX} was calculated by using Eqs. (2), (4), and (5), where

$$P_0 = 1 - P_-[T=T_{AF}, t=\delta, n=1, P_0=P_\infty(T_B^{set})], \quad (8)$$

the temperature T_{AF} being varied until $H_{EX}=H_{EX}^W=0$ Oe was fulfilled, corresponding to $T_{AF}=T_{AF}^W$. The dependence $T_{AF}^W(\delta)$ calculated by this method is shown by the solid line in Fig. 2(b). Agreement over a large interval of pulse widths, extending from 20 ns to 1 s, was obtained between the result of HDE simulations using bulk values for the thermodynamic parameters of the junction layers and the result of the A-N regarding the temperature of the AF layer at $t=\delta$. As one can notice in Fig. 2(b) the A-N model indicates lower values for T_{AF}^W than the HDE simulations for $\delta<20$ ns. This discrepancy was ascribed to the failure of the rectangular temperature pulse assumption for pulse widths having the same order of magnitude as the intrinsic heating/cooling times required by the junction to reach a stationary temperature regime. Therefore, in a second step, in order to correctly account for the transient heating/cooling regimes, the A-N model was modified to calculate H_{EX} at the end of an arbitrarily shaped temperature pulse $T_{AF}(t)$. The time dependence of the AF temperature during and after the application of an electric pulse of power P_{HP}^W and width δ, $T_{AF}(t)$, was calculated by HDE simulations [Fig. 5(a)], and then introduced in the A-N model to calculate H_{EX} at the end of the pulse. In order to calculate $P_-(t)$, required by Eq. (8), we have solved the Master equation[9,10]

$$\frac{dP_-}{dt} = -f_0 P_- \exp[-\Delta E_+] + (1-P_-)\exp[-\Delta E_-] \quad (9)$$

by taking into account the temperature profile $T_{AF}(t)$ and the initial condition $P_-(t=0)=1-P_\infty(T_B^{set})$. The solution of Eq. (9) at the end of the temperature pulse $T_{AF}(t-\delta \cong 15$ ns) was used in Eq. (8) and then in Eqs. (4) and (5) for calculating

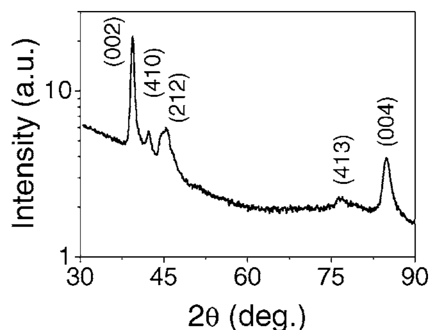

FIG. 6. XRD spectra of a 50 nm Ta layer, indicating the dominance of the β-Ta tetragonal phase.

H_{EX} and H_C from Eqs. (2) and (3). The temperature pattern $T_{AF}(t)$ was normalized to $T_{AF}(t=\delta)$ which was varied until the writing condition $H_{EX}=H_{EX}^W=0$ Oe was fulfilled. The corresponding normalization factor was $T_{AF}(t=\delta)=T_{AF}^W(\delta)$. The dependence $T_{AF}^W(\delta)$ obtained using this approach is plotted in Fig. 2(b) for $\delta=2-100$ ns. From Fig. 2(b) one can notice that this approach considerably improves the agreement between HDE, and A-N model results in the range of short pulse widths of 2–20 ns, giving similar results with the previous approach for pulse widths δ larger than the intrinsic heating/cooling times of the junction. The matching between the HDE thermodynamic simulations and the A-N magnetic calculations illustrated in Fig. 2(b) evidences an increase of T_B by almost 80% when the electric pulse duration decreases from 1 s down to 2 ns. As a consequence of thermal relaxation in the AF layer, the shorter the heating pulse the closer is the writing temperature to T_N of the AF layer. This suggests that the writing energy could be significantly reduced by selecting an AF material with a low T_N.

For the investigated device, the application of high temperature pulses, as required for writing with short electric pulses of width δ in the nanosecond range [Fig. 2(a)], was enabled by the presence in the MTJ stack of layers with low thermal conductivity, playing the role of thermal barriers. Figure 5(b) shows the MTJ temperature profile created by an electric pulse of power $P_{HP}^W(\delta=16\text{ ns})=2.71$ mW, at $t=\delta$. The most important contribution to the retention of heat in the MTJ comes from the Ta layers placed at the bottom and top of the junction. The low thermal conductivity of the Ta layers, $k=4.3$ W/K/m, is characteristic of the β-Ta phase,[13–15] predominant in our Ta films as suggested by the high electrical resistivity $\rho_e=170$ $\mu\Omega$ cm and by the x-ray diffraction (XRD) data (Fig. 6). The introduction of thermal barriers on both sides of the MTJ improves the heating efficiency and reduces the energy necessary per write event.

CONCLUSIONS

In thermally assisted MRAM, the exchange bias acting on the storage layer is set by heating the junction with an electric pulse. The dependence of the electric pulse power required to set the exchange bias to a specific threshold $H_{EX}=H_{EX}^W=0$ Oe on its duration was experimentally established. A method to determine the temperature T_{AF} reached by the AF layer during the application of a heating electric pulse was proposed. The relationship $T_{AF}(\delta)$ leading to the same threshold of exchange bias was obtained over a large window of heating times δ ranging from 2 ns to 1 s. Two approaches were proposed for this purpose and their results were compared. The first approach is based on the resolution of the heat diffusion equation for all the layers of the device. This approach assumed that the experimental power of the heating pulse was converted into heat in the tunnel barrier by Joule effect, allowing a direct knowledge of the heat source term in the heat diffusion equation. A second approach is based on the interpretation of the experimental dependence of the exchange bias H_{EX} on the duration of the heating pulse by an A-N model of exchange bias. These two approaches suggest an increase of the AF temperature required for writing by almost 80% when the electric pulse duration decreases from 1 s down to 2 ns. As suggested by the A-N model, this effect is a consequence of thermal relaxation in the AF layer. This temperature increase is enabled by the use of layers having low thermal conductivities, playing the role of thermal barriers, placed on both sides of the tunnel junction.

ACKNOWLEDGMENTS

We thank A. Astier and O. Redon for sample fabrication at CEA-LETI, E. Gautier for SEM work, and B. Rodmacq for XRD measurements. This work was supported by the European RTN SPINSWITCH (MRTN-CT-2006-035327).

[1] J. Nogues and I. K. Schuller, J. Magn. Magn. Mater. **192**, 203 (1999).
[2] A. E. Berkowitz and K. Takano, J. Magn. Magn. Mater. **200**, 552 (1999).
[3] J. C. S. Kools, IEEE Trans. Magn. **32**, 3165 (1996).
[4] J. Wang and P. P. Freitas, Appl. Phys. Lett. **84**, 945 (2004).
[5] R. C. Sousa, M. Kerekes, I. L. Prejbeanu, O. Redon, B. Dieny, J. P. Nozieres, and P. P. Freitas, J. Appl. Phys. **99**, 08N904 (2006).
[6] J. G. Deak, J. M. Daughton, and A. V. Pohm, IEEE Trans. Magn. **42**, 2721 (2006).
[7] I. L. Prejbeanu, M. Kerekes, R. C. Sousa, H. Sibuet, O. Redon, B. Dieny, and J. P. Nozieres, J. Phys.: Condens. Matter **19**, 165218 (2007).
[8] See http://www.webelements.com for thermal conductivity k, molar heat capacity C_M, molar volume V_M, and density δ for Al, Cu, and Ru.
[9] E. Fulcomer and S. H. Charap, J. Appl. Phys. **43**, 4190 (1972).
[10] K. Nishioka, C. Hou, H. Fujiwara, and R. Metzger, J. Appl. Phys. **80**, 4528 (1996).
[11] K. Nishioka, S. Shigematsu, T. Imagawa, and S. Narishige, J. Appl. Phys. **83**, 3233 (1998).
[12] H. Xi, R. M. White, Z. Gao, and S. Mao, J. Appl. Phys. **92**, 4828 (2002).
[13] J. Narayan, V. Bhosle, A. Tiwari, A. Gupta, P. Kumar, and R. Wu, J. Vac. Sci. Technol. A **24**, 1948 (2006).
[14] J. J. Senkevich, T. Karabacak, D.-L. Bae, and T. S. Cale, J. Vac. Sci. Technol. B **24**, 534 (2006).
[15] A. Jiang, T. A. Tyson, L. Axe, L. Gladczuk, M. Sosnowski, and P. Cote, Thin Solid Films **479**, 166 (2005).

Journal of Applied Physics is copyrighted by the American Institute of Physics (AIP). Redistribution of journal material is subject to the AIP online journal license and/or AIP copyright. For more information, see http://ojps.aip.org/japo/japcr/jsp